Journal of Sensor Science and Technology
Vol. 31, No. 4 (2022) pp. 187-193
http://dx.doi.org/10.46670/JSST.2022.31.4.187
pISSN 1225-5475/eISSN 2093-7563

Nanocatalyst Decorated Metal Oxides on Highly Selective Chemical Sensors

Ji-Won Jung[1,+] and Ji-Soo Jang[2,+]

Abstract

The accurate detection of environmental and biomarker gas species has attracted increasing attention due to their broad applications, such as air quality monitoring, disease diagnosis, and explosive chemicals detection. To accurately detect target gas species using chemiresistive gas sensors, using nanocatalysts on semiconducting metal oxides (SMOs) is considered the most promising approach. This review summarizes recent studies on methods for nanocatalysts functionalization on SMOs to achieve the highly selective gas sensors. To this end, we discuss various nanocatalyst decorated metal oxide-based chemiresistive gas sensors and provide an insight to construct highly accurate gas sensors.

Keywords: Gas sensors, Oxide semiconductors, Nanocatalysts

1. NANOCATALYSTS ON METAL OXIDES FOR SELECTIVE GAS SENSING

Since the discovery of their gas sensing property in the early 1960s, semiconducting metal oxides0(SMOs) have been investigated for gas detector applications [1]. SMOs based chemiresistive sensors have been receiving increasing attention because of their extensive applications in monitoring air pollution, toxic and flammable gases, food conditions, and medical diagnosis [2-6]. Particularly, because SMO-based gas sensors exhibit simple operation, low cost, fast response, ease of miniaturization, and outstanding limit of detection, designing SMO-based gas sensors is promising for practical use [7,8]. However, low selectivity to target gas molecules remains a critical barrier for practical use. As a promising approach for boosting the selectivity of SMOs gas sensors, the functionalization of nanocatalysts on the surface of SMOs is an important technology[9].

For example, Jang et al. reported that uniformly decorating Pt on SnO_2 nanotubes employing bio-inspired nanocatalysts could significantly improve the selectivity of sub-ppm level acetone gas molecules [10]. Shin et al. developed a single Pt atom loaded SnO_2 nanofiber for highly selective H_2S detection [11]. Conventional synthetic methods for nanocatalyst decoration on desired SMO support materials; however, these methods do not allow simultaneous manipulation of several critical factors of SMO-based gas sensors, such as grain size, pore, size, and nanocatalyst uniformity on SMO supports. This review summarizes the effective nanocatalysts functionalization methods regarding desired SMOs, such as templating route, thermal-shock methods, and photo-thermal methods. In each part, we highlight the different nanocatalysts functionalization methods with high uniformity and small size. We hope that this review can effectively guide and stimulate various creative ideas that can revolutionize accurate gas sensors.

2. BIO-INSPIRED NANOCATALYST DECORATION ON METAL OXIDE NANOFIBERS

Apoferritin is a family of iron storage proteins composed of 24 protein subunits, which have approximately 12–13 nm exterior diameter with an inner cavity of 7–8 nm [12,13]. Apoferritin is a promising nano-template for synthesizing nanoparticles due to its unique hollow nanostructure. As shown in Fig. 1a, the inorganic cations in an aqueous solution can infiltrate into the core of apoferritin through its 3-fold axis; subsequently, the reduction of inner side cations can be reduced by sodium borohydride [14,15]. Therefore, sub-10 nm-sized metallic nanoparticles can be

[1]School of Materials Science and Engineering, University of Ulsan (UOU), 12, Technosaneop-ro 55beon-gil, Nam-gu, Ulsan 44776, Republic of Korea
[2]Electronic Materials Research Center, Korea Institute of Science and Technology, 5, Hwarang-ro 14-gil, Seongbuk-gu, Seoul 02792, Republic of Korea
[+]Corresponding author: jwjung4@ulsan.ac.kr, wkdwltn92@kist.re.kr
(Received: Jun. 23, 2022, Revised: Jul. 10, 2022, Accepted: Jul. 16, 2022)

encapsulated in the apoferritin. Through the transmission electron microscopy (TEM) analysis, the Pt, Pd, and Rh nanoparticles (NPs) encapsulated in apoferritin can be clearly observed (Figs. 1b–d). Because the apoferritin template encapsulates the metallic NPs, sub-10 nm metallic NPs can be uniformly formed. Such apoferritin encapsulated metallic NPs demonstrated excellent dispersibility in deionized (DI) water. Therefore, these NP solutions can be easily dispersed in an electrospinning solution, enabling the functionalization of metallic NPs on electrospun nanofibers. Then, the subsequent calcination of metallic NPs loaded electrospun nanofibers induces the formation of metallic NPs loaded metal oxide nanofibers. As shown in Fig. 1e, Pt NP-loaded WO_3 nanofibers are formed with uniform nanofiber width. Moreover, we realized that the burn-out of organic apoferritin can induce numerous pores on WO_3 nanofibers as shown in Figs. 1f and 1g. Furthermore, owing to the excellent dispersibility of apoferritin-based catalytic NPs, Pt NPs are well-distributed on the WO_3 nanofibers (Fig. 1h).

By controlling the catalytic NPs on WO_3 nanofibers, such as the Pt-WO_3 nanofibers, Pd-WO_3 nanofibers, and Rh-WO_3 nanofibers, the selective detection capability can be manipulated. For example, Pt-WO_3 nanofibers show exceptional selectivity to acetone, while Pd- and Rh-loaded WO_3 nanofibers show selectivity to toluene and H_2S, respectively (Figs. 1i–1k). It means that tuning catalytic NPs on WO_3 nanofibers can induce different selectivity to target gas molecules. Based on these results, the bio-template (i.e., apoferritin) driven catalytic NPs can be uniformly functionalized on electrospun metal oxide nanofibers; accordingly, the bio-template can induce porosity on metal oxide nanofibers. Therefore, the sensitivity and selectivity to target gas molecules are simultaneously boosted.

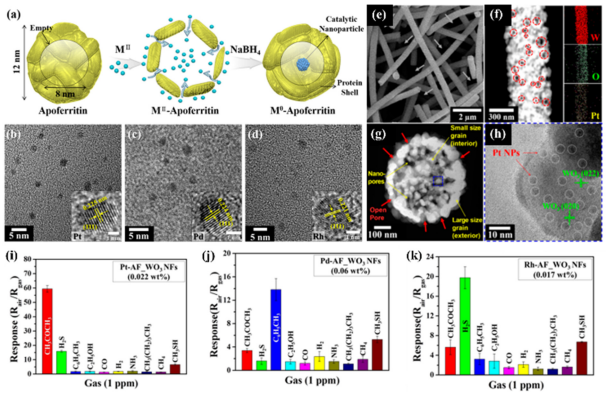

Fig. 1. (a) Illustration of the synthetic strategy for nanocatalyst encapsulation in apoferritin. TEM images of (b) Pt nanoparticles encapsulated in apoferritin (AF-Pt NPs), (c) AF-Pd NPs, and (d) AF-Rh NPs. (e) SEM image of Pt loaded WO_3 nanofibers (Pt-WO_3 NFs), (f) STEM images of Pt-WO_3 NFs with EDS mapping results, (g) cross-sectional STEM image of Pt-WO_3 NFs, and (h) high-resolution TEM image of Pt-WO_3 NFs. Selectivity property of (i) Pt-WO_3 NFs, (j) Pd-WO_3 NFs, and (k) Rh-WO_3 NFs [14]

3. IN-SITU NANOCATALYST GROWTH TECHNIQUE ON METAL OXIDES: EX-SOLUTION

In addition to bio-template-based nanocatalysts, in-situ nanocatalyst growth technique on desired host oxides, called “ex-solution”, have attracted attention as an intriguing route to obtaining highly stable nanocatalysts [16]. It is based on the phenomenon that specific cations in the desired oxide lattice selectively precipitate on the host oxide surface when the host oxide is reduced at a high temperature [17]. The metal NPs synthesized by the ex-solution process are strongly bound to the host oxide; thus, they exhibit outstanding thermal and chemical stability. As shown in Fig. 2a, the Ir NPs on the WO_3 host oxide can be formed by the phase transition of host oxide [18]. Starting from Ir-doped WO_3 nanosheets, the elevated temperature in H_2/Ar gas atmosphere induce the in-situ growth

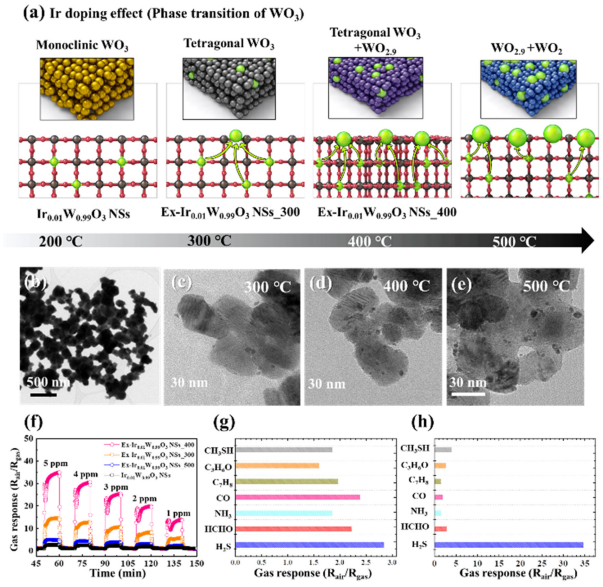

Fig. 2. (a) Schematics of the synthetic ex-soultion process of Ir catalysts on WO_3 nanosheets under various conditions. In situ TEM images of Ir doped WO_3 nanosheets under reduced gas atmosphere at various temperatures: (b) room temperature, (c) 300°C, (d) 400°C, (e) 500°C. (f) dynamic H_2S response transitions of Ir nanoparticles with ex-solved WO_3 nanosheets (1–5 ppm), selectivity properties of (g) Ir doped WO_3 nanosheets, and (h) Ir nanoparticles with ex-solved WO_3 nanosheets [18]

of Ir NPs on WO_3 nanosheets. Due to the phase transition of WO_3 (monoclinic → tetragonal → $WO_{2.9}$ → WO_2), the inner side Ir dopants can be extracted from the host oxides, forming the Ir NPs on the WO_3 nanosheets. The Ir-doped WO_3 nanosheets at room temperature do not exhibit Ir NP formation, while Ir doped WO_3 nanosheets at 300°C exhibit small Ir NP formation; elevated temperatures induce highly-dense NPs with large size on host oxide (Fig. 2b–2e). Because the Ir NPs with ex-solved WO_3 nanosheets exhibit high uniformity and strong bonding energy with WO_3 nanosheets, they possess outstanding sensitivity with high stability (Fig. 2f). Notably, Ir-doped WO_3 nanosheets exhibit poor selectivity to target gas molecules, while Ir NPs with ex-solved WO_3 nanosheets exhibit exceptional H_2S sensing selectivity (Fig. 2g and 2h). This means that ex-solved catalytic NPs on host oxides can boost the sensing selectivity to target gas molecules. Considering the numerous advantages of ex-solved NPs, such as strong durability, excellent selectivity, and high dispersibility on host oxide, the ex-solution technique can be further applied to chemiresistive sensing fields.

4. MOFS DERIVED NANOCATALYST DEPOSITION ON METAL OXIDES

Metal-organic frameworks (MOFs) have attracted increasing attention owing to their intriguing features, such as significant surface area, ultrahigh porosity, and adaptability to various structures [19-21]. In particular, their ability to encapsulate catalytic NPs, such as Pt, Pd, and Au, within their cavities has been considered a noteworthy feature. For example, Hermes et al. reported that metal-loaded MOFs release metallic atoms from their precursors using metal-organic chemical vapor deposition [22]. Likewise, MOFs are an effective sacrificial template for encapsulating the tiny nanocatalysts and can be transferred to desired oxide structures. As shown in Fig. 3a, the Pd cations can be diffused into the inner side pores in ZIF-8; subsequently, the chemical reduction using $NaBH_4$ can induce the creation of catalytic Pd NP-loaded ZIF-8 [23]. Through the TEM analysis, sub-5 nm Pd NPs are successfully encapsulated in ZIF-8 (Fig. 3b and 3c). Owing to the space limitation of pores in ZIF-8, significantly small-sized Pd NPs can be formed on ZIF-8. These nanocatalysts loaded ZIF-8 can be simply dispersed in the electrospinning solution (e.g., DMF solvent). Thus, such catalyst-loaded ZIF-8 can be loaded on the electrospun nanofibers, which have metal oxide precursors,

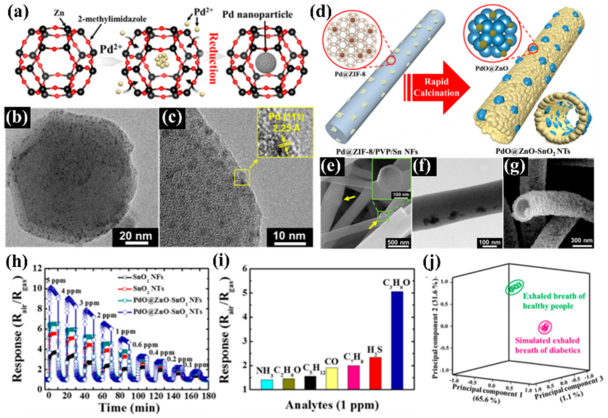

Fig. 3. (a) Illustration of the encapsulation process of Pd nanoparticles in ZIF-8, (b–c) TEM images of Pd nanoparticles encapsulated ZIF-8. (d) Illustration of the synthetic process for PdO catalysts loaded SnO_2 nanotubes, (e) SEM image and (f) TEM image of the Pd@ZIF-8 loaded as-spun nanofiber, and (g) SEM image of the PdO catalysts loaded SnO_2 nanotubes. (h) Dynamic acetone gas response transition and (i) selectivity characteristics of SnO_2 nanotubes based sensors. (j) Pattern recognition of exhaled breath of simulated diabetic patients and healthy people using PCA analysis [23, 24]

polymer, and nanocatalyst loaded ZIF-8 (Fig. 3d). As shown in Figs. 3e and 3f, the nanocatalyst loaded ZIF-8 is successfully loaded on as-spun nanofibers. After the calcination process of these electrospun nanofibers, nanocatalysts in ZIF-8 are loaded on the SnO_2 nanotubes; accordingly, ZIF-8 change to ZnO particles [24]. Finally, the nanocatalysts loaded ZnO/SnO_2 composite nanotubes are formed (Fig. 3g). Owing to the uniform distribution of PdO nanocatalysts on ZnO/SnO_2 composite nanotubes and heterogeneous nanostructures, the PdO NPs loaded ZnO/SnO_2 composite nanotubes demonstrate high acetone responses as well as excellent selectivity to acetone (Fig. 3h and 3i). Based on the significant acetone selectivity of the PdO NPs loaded ZnO/SnO_2 composite nanotubes, PdO NPs loaded ZnO/SnO_2 composite nanotubes can be utilized to distinguish between diabetic patients and healthy people with exhalation experiments; note that the acetone gas species in human breath is related with diabetic patients. In this sense, we can realize that the numerous pore sites in MOFs can be used as encapsulation sites for nanocatalysts. These catalytic NPs in MOFs are loaded onto the desired oxide supports to boost up the selectivity to target gas molecules. However, after the calcination of nanocatalysts loaded MOFs, the MOFs driven residue oxides should be left in the composite materials. Therefore, it is hard to decorate the pure metallic nanocatalysts on desired oxides using the MOF templating approach.

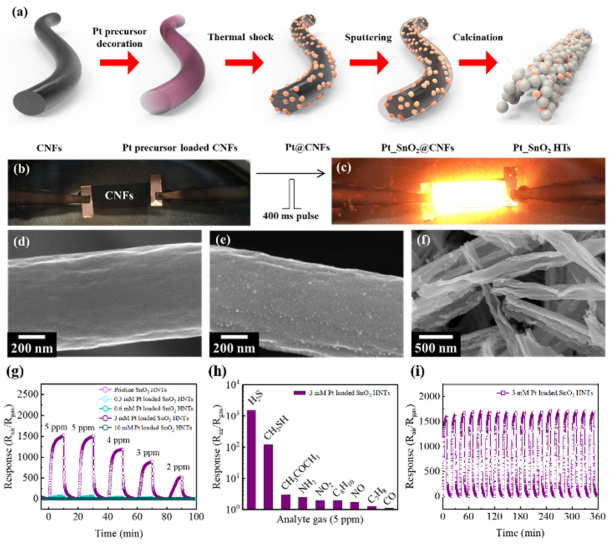

Fig. 4. (a) Illustration of synthesis of Pt decorated CNFs and Pt decorated SnO_2 hemitubes. Digital images of CNFs paper (b) before thermal shock, and (c) during thermal shock. SEM images of (d) CNFs, (e) Pt decorated CNFs, and (f) Pt decorated SnO_2 hemitubes. (g) Dynamic H_2S sensing response of Pt loaded SnO_2 hemitubes samples at 300°C, (h) selectivity property of Pt loaded SnO_2 hemitubes, and (i) sensing stability test results of Pt loaded SnO_2 hemitubes toward 5 ppm H_2S (18 cycles)[29]

5. THERMAL SHOCK-DERIVED NANOCATALYSTS DECORATION ON HOLLOW METAL OXIDES

Another promising approach for the functionalization of nanocatalysts on the oxides is the thermal-shock method [25,26]. Utilizing joule-heating with ultrafast pulse thermal shock (400 ms) on the conductive carbon materials, a temperature over 1000 K can be emitted on the conductive carbon materials. Using such a phenomenon, metal precursors loaded on the conductive carbon materials can be transited to tiny metal NPs on the conductive carbon materials with high uniformity through fission and fusion mechanisms [27,28]. For example, as shown in Fig. 4a, the electrospinning-driven carbon nanofibers (CNFs) can be easily coated by metal precursors using dip-coating or drop coating methods[29].

After that, the subsequent thermal-shock process under vacuum induces the formation of catalytic NPs on the CNFs (Figs. 4d and 4e). Owing to the rapid thermal-shock process (< 400 ms), significantly small-sized Pt NPs are uniformly decorated on the CNFs. Owing to the high temperature during the thermal shock, the shining light forms on the CNFs membrane (Figs. 4b and 4c). To transfer the as-prepared catalysts onto the desired oxide supports, physical vapor deposition methods, such as sputtering, can be employed. For example, the SnO_2 layer is decorated onto the Pt-loaded CNFs, and subsequent heat-treatment at ambient air induces the creation of Pt catalyst-loaded SnO_2 hemitubes (Fig. 4f). Because the thermal-shock process is conducted under high vacuum conditions, pure metallic Pt NPs were formed on the CNFs, thus enabling to transfer the high-quality Pt NPs onto the desired host oxides with high uniformity. The H_2S sensing tests are carried out using thermal-shock process-driven Pt decorated SnO_2 hemitubes. As shown in Fig. 4g, Pt decorated SnO_2 hemitubes exhibit exceptional high response to ppm level H_2S (1–5 ppm). Furthermore, the selectivity of Pt decorated SnO_2 hemitubes for H_2S or CH_3SH is outstanding. Because the H_2S or CH_3SH gas molecules are key bio-markers for halitosis patients, thermal shock-driven Pt-loaded SnO_2 hemitubes can be potentially utilized in breath analyzers [30]. Regarding catalyst stability, Pt-loaded SnO_2 hemitubes demonstrate high recyclability with respect to repetitive H_2S sensing cycles. This means that catalytic Pt NPs on SnO_2 hemitubes maintained their size, uniformity, and metallic status.

6. INTENSE-PULSE LIGHT (IPL) BASED NANOCATALYST DEPOSITION ON METAL OXIDES

The light-based synthetic tools, such as intense-pulse light (IPL), have attracted attention owing to their fast synthesis time, minimal material degradation, and high reproducibility [31-33]. When an oxide sample is irradiated with high-energy light, the incident photons can interact with the electrons inside the oxides, resulting in a photothermal energy transfer. Therefore, the temperature of the desired oxide can be rapidly increased over 1000°C, resulting in the oxide phase transition or catalyst functionalization on host oxides. Fig. 5a indicates that the metal precursor-loaded oxide samples can be transited to metal NPs loaded metal oxides. When the aqueous metal precursors loaded SnO_2 nanosheets are irradiated from IPL, the momentary thermal shock is emitted to SnO_2 nanosheets. Therefore, the metal ions can be reduced to metallic NPs on the host oxides. As shown in Fig. 5b, regarding the SnO_2 nanosheets, the momentary temperature of SnO_2 nanosheets reached over 1500°C within 20 ms. Owing to the ultra-fast heating rate, the degradation of SnO_2 exceeding grain growth is prevented, while PtRu, PtIr, or PtRuIr NPs are successfully decorated on the SnO_2 nanosheets (Figs. 5c–5e). The

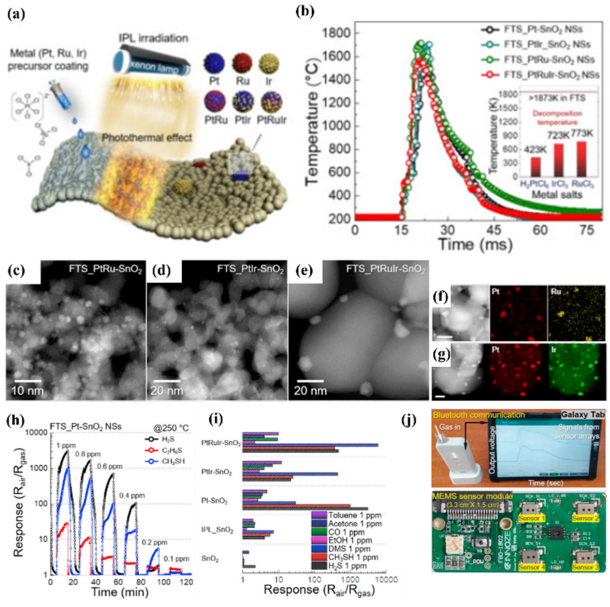

Fig. 5. (a) Illustrations of synthesis of metal oxide nanosheets stabilized by nanocatalsts via IPL treatment. (b) Temperature-time curves of metal precursors loaded SnO_2 nanosheets with IPL treatment. STEM images of (c) PtRu loaded SnO_2 nanosheets, (d) PtIr loaded SnO_2 nanosheets, and (e) PtRuIr loaded SnO_2 nanosheets. STEM elemental maps of (f) PtRu loaded SnO_2 nanosheets and (g) PtIr loaded SnO_2 nanosheets. (h) Sensing results of Pt loaded SnO_2 nanoheets regarding H_2S, CH_3SH, and C_2H_6S at 250°C, (i) selective sensing characteristics of Pt loaded SnO_2 nanoheets, and (j) digital images of portable MEMS device and MEMS sensor module [31]

formation of polyelemental NPs on SnO_2 nanosheets is also demonstrated using STEM elemental mapping analysis (Figs. 5f and 5g). The polyelemental nanocatalysts on host oxides can further enhance the catalytic effect compared with that of single component catalysts, resulting in exceptional sensing performances. The gas sensing measurement i carried out using the IP-treated Pt-loaded SnO_2 nanosheet samples. Interestingly, IPL-treated Pt-loaded SnO_2 nanosheets exhibited over 1000 H_2S sensing response (R_{air}/R_{gas}) even under 1 ppm level H_2S (Fig. 5h). Furthermore, IPL treatment induces the generation of high-quality metallic NPs on the oxides; which conventionally demonstrate selectivity to sulfur compounds (Fig. 5i). To generate the IPL-treated nanocatalysts-loaded oxide sensing devices, the MEMS sensor platform is employed with Bluetooth communication between tab and portable sensing devices (Fig. 5j).

7. CONCLUSIONS

In this comprehensive review, we introduced various methods for functionalizing nanocatalysts on host oxides with high uniformity, constant size distribution, and strong interactions between oxides and nanocatalysts. As the unique nanocatalyst decoration techniques on metal oxides, the bio-inspired protein cage (apoferritin), MOFs templating routes, thermal-shock joule heating, and photothermal tool were summarized in this review. In addition to single component catalytic NPs (e.g., Pt, Pd, Rh, and Ni), polyelemental NPs (e.g., PtPd, PtNi, and PtRh) were synthesized and decorated onto the metal oxides to identify their exceptional catalytic activities. Nanocatalysts decorated metal oxide-based chemiresistors have been intensively studied in recent years. However, further improvements are still needed to utilize such materials in commercial sensors over a wide range of applications. (1) Nanocatalysts should be uniformly decorated on the metal oxide to achieve highly reliable sensing properties with high sensitivity and selectivity. (2) The density of nanocatalysts on the oxide should be optimized to minimize sensor degradation. Moreover, establishing the interactions between nanocatalysts and gas species, reaction kinetics, and thermodynamic mechanisms is crucial. These points can be addressed by various nanocatalyst functionalization tools. We hope that this review effectively paves the way for the commercial application of nanocatalysts-loaded metal oxides chemiresistive sensors.

ACKNOWLEDGMENT

J.S.J. acknowledges support from KIST (2E31771). This research was supported by a National Research Foundation of Korea (NRF) grant funded by the Korean government (MSIT: Ministry of Science and ICT)(NRF-2021R1F1A1060285).

REFERENCES

[1] S. J. Kim, S. J. Choi, J. S. Jang, H. J. Cho, and I. D. Kim, "Innovative nanosensor for disease diagnosis", *Acc. Chem. Res.*, Vol. 50, No. 7, pp. 1587-1596, 2017.

[2] J. S. Jang, S. J. Choi, S. J. Kim, M. Hakim, and I. D. Kim, "Rational design of highly porous SnO2 nanotubes functionalized with biomimetic nanocatalysts for direct observation of simulated diabetes", *Adv. Funct. Mater.*, Vol. 26, No. 26, pp. 4740-4748, 2016.

[3] J. S. Jang, L. R. Winter, C. Kim, J. D. Fortner, and M. Elimelech, "Selective and sensitive environmental gas sensors enabled by membrane overlayers", *Trends Chem.*, Vol. 3, No. 7, pp. 547-560, 2021.

[4] J. S. Jang, H. J. Jung, S. Chong, D. H. Kim, J. Kim, S. O. Kim, and I. D. Kim, "2D materials decorated with ultrathin

and porous graphene oxide for high stability and selective surface activity", *Adv. Mater.*, Vol. 32, No. 36, p. 2002723, 2020.

[5] J. S. Jang, J. Lee, W. T. Koo, D. H. Kim, H. J. Cho, H. Shin, and I. D. Kim, "Pore-size-tuned graphene oxide membrane as a selective molecular sieving layer: toward ultraselective chemiresistors", *Anal. Chem.*, Vol. 92, No. 1, pp. 957-965, 2019.

[6] J. Lee, D. Cho, H. Chen, Y. S. Shim, J. Park, and S. Jeon, "Proximity-field nanopatterning for high-performance chemical and mechanical sensor applications based on 3D nanostructures", *Appl. Phys. Rev.*, Vol. 9, No. 1, p. 011322, 2022.

[7] D. Cho, J. M. Suh, S. H. Nam, S. Y. Park, M. Park, T. H. Lee, K. S. Choi, J. Lee, C. Ahn, and H. W. Jang, "Optically Activated 3D Thin-Shell TiO2 for Super-Sensitive Chemoresistive Responses: Toward Visible Light Activation", *Adv. Sci.*, Vol. 8, No. 3, p. 2001883, 2021.

[8] J. M. Suh, D. Cho, S. Lee, T. H. Lee, J. W. Jung, J. Lee, S. H. Cho, T. H. Eom, J. W. Hong, and Y. S. Shim, "Rationally designed TiO2 nanostructures of continuous pore network for fast-responding and highly sensitive acetone sensor", *Small Methods*, Vol. 5, No. 12, p. 2100941, 2021.

[9] C. Park, W. T. Koo, S. Chong, H. Shin, Y. H. Kim, H. J. Cho, J. S. Jang, D. H. Kim, J. Lee, and S. Park, "Confinement of Ultrasmall Bimetallic Nanoparticles in Conductive Metal–Organic Frameworks via Site-Specific Nucleation", *Adv. Mater.*, Vol. 33, No. 38, p. 2101216, 2021.

[10] J. S. Jang, S. J. Kim, S. J. Choi, N. H. Kim, M. Hakim, A. Rothschild, and I. D. Kim, "Thin-walled SnO2 nanotubes functionalized with Pt and Au catalysts via the protein templating route and their selective detection of acetone and hydrogen sulfide molecules", *Nanoscale*, Vol. 7, No. 39, pp. 16417-16426, 2015.

[11] H. Shin, W. G. Jung, D. H. Kim, J. S. Jang, Y. H. Kim, W. T. Koo, J. Bae, C. Park, S. H. Cho, and B. J. Kim, "Single-atom Pt stabilized on one-dimensional nanostructure support via carbon nitride/SnO2 heterojunction trapping", *ACS Nano*, Vol. 14, No. 9, pp. 11394-11405, 2020.

[12] Z. Yang, X. Wang, H. Diao, J. Zhang, H. Li, H. Sun, and Z. Guo, "Encapsulation of platinum anticancer drugs by apoferritin", *Chem. Commun.*, Vol. 33, pp. 3453-3455, 2007.

[13] Y. Shin, A. Dohnalkova, and Y. Lin, "Preparation of homogeneous gold− silver alloy nanoparticles using the apoferritin cavity as a nanoreactor", *J. Phys. Chem. C*, Vol. 114, No. 13, pp. 5985-5989, 2010.

[14] S. J. Kim, S. J. Choi, J. S. Jang, N. H. Kim, M. Hakim, H. L. Tuller, and I. D. Kim, "Mesoporous WO3 nanofibers with protein-templated nanoscale catalysts for detection of trace biomarkers in exhaled breath", *ACS Nano*, Vol. 10, No. 6, pp. 5891-5899, 2016.

[15] S. J. Choi, S. J. Kim, H. J. Cho, J. S. Jang, Y. M. Lin, H. L. Tuller, G. C. Rutledge, and I. D. Kim, "WO3 nanofiber-based biomarker detectors enabled by protein-encapsulated catalyst self-assembled on polystyrene colloid templates", *Small*, Vol. 12, No. 7, pp. 911-920, 2016.

[16] J. H. Kim, J. K. Kim, J. Liu, A. Curcio, J. S. Jang, I. D. Kim, F. Ciucci, and W. Jung, "Nanoparticle ex-solution for supported catalysts: materials design, mechanism and future perspectives", *ACS Nano*, Vol. 15, No. 1, pp. 81-110, 2020.

[17] D. Neagu, T. S. Oh, D. N. Miller, H. Ménard, S. M. Bukhari, S. R. Gamble, R. J. Gorte, J. M. Vohs, and J. T. "Irvine, Nano-socketed nickel particles with enhanced coking resistance grown in situ by redox exsolution", *Nat. Commun.*, Vol. 6, No. 1, pp. 1-8, 2015.

[18] J. S. Jang, J. K. Kim, K. Kim, W. G. Jung, C. Lim, S. Kim, D. H. Kim, B. J. Kim, J. W. Han, and W. Jung, "Dopant-Driven Positive Reinforcement in Ex-Solution Process: New Strategy to Develop Highly Capable and Durable Catalytic Materials", *Adv. Mater.*, Vol. 32, No. 46, p. 2003983, 2020.

[19] J. S. Jang, W. T. Koo, S. J. Choi, and I. D. Kim, "Metal organic framework-templated chemiresistor: sensing type transition from P-to-N using hollow metal oxide polyhedron via galvanic replacement", *J. Am. Chem. Soc.*, Vol. 139, No. 34, pp. 11868-11876, 2017.

[20] W. T. Koo, J. S. Jang, and I. D. Kim, "Metal-organic frameworks for chemiresistive sensors", *Chem*, Vol. 5, No. 8, pp. 1938-1963, 2019.

[21] M. G. Campbell, S. F. Liu, T. M. Swager, and M. Dinca, "Chemiresistive sensor arrays from conductive 2D metal–organic frameworks", *J. Am. Chem. Soc.*, Vol. 137, No. 43, pp. 13780-13783, 2015.

[22] S. Hermes, F. Schröder, S. Amirjalayer, R. Schmid, and R. A. Fischer, "Loading of porous metal–organic open frameworks with organometallic CVD precursors: inclusion compounds of the type [L n M]a@ MOF-5", *J. Mater. Chem.*, Vol. 16, No. 25, pp. 2464-2472, 2006.

[23] W. T. Koo, S. J. Choi, S. J. Kim, J. S. Jang, H. L. Tuller, and I. D. Kim, "Heterogeneous sensitization of metal–organic framework driven metal@ metal oxide complex catalysts on an oxide nanofiber scaffold toward superior gas sensors", *J. Am. Chem. Soc.*, Vol. 138, No. 40, pp. 13431-13437, 2016.

[24] W. T. Koo, J. S. Jang, S. J. Choi, H. J. Cho, and I. D. Kim, "Metal–organic framework templated catalysts: dual sensitization of PdO–ZnO composite on hollow SnO2 nanotubes for selective acetone sensors", *ACS Appl. Mater & Interfaces*, Vol. 9, No. 21, pp. 18069-18077, 2017.

[25] W. B. Jung, H. Park, J. S. Jang, D. Y. Kim, D. W. Kim, E. Lim, J. Y. Kim, S. Choi, J. Suk, and Y. Kang, "Polyelemental nanoparticles as catalysts for a Li–O2 battery", *ACS Nano*, Vol. 15, No. 3, pp. 4235-4244, 2021.

[26] J. Y. Song, C. Kim, M. Kim, and K. M. Cho, "I. Gereige, W. B. Jung, H. Jeong, and H. T. Jung, "Generation of high-density nanoparticles in the carbothermal shock method", *Sci. Adv.*, Vol. 7, No. 48, p. eabk2984, 2021.

[27] Y. Yao, Z. Huang, P. Xie, S. D. Lacey, R. J. Jacob, H. Xie, F. Chen, A. Nie, T. Pu, and M. Rehwoldt, "Carbothermal shock synthesis of high-entropy-alloy nanoparticles", *Science*, Vol. 359, No. 6383, pp. 1489-1494, 2018.

[28] M. Wu, M. Cui, L. Wu, S. Hwang, C. Yang, Q. Xia, G. Zhong, H. Qiao, W. Gan, and X. Wang, "Hierarchical poly-elemental nanoparticles as bifunctional catalysts for oxygen evolution and reduction reactions", *Adv. Energy Mater.*, Vol.

10, No. 25, p. 2001119, 2020.
[29] S. Chae, J. Ahn, J.S. Nam, J. S. Jang, and I. D. Kim, "Thermal shock-stabilized metal catalysts on oxide hemitubes: Toward ultrasensitive chemiresistors", *Appl. Surf. Sci.*, Vol. 595, p. 153460, 2022.
[30] H. Shin, D. H. Kim, W. Jung, J. S. Jang, Y. H. Kim, Y. Lee, K. Chang, J. Lee, J. Park, and K. Namkoong, "Surface activity-tuned metal oxide chemiresistor: toward direct and quantitative halitosis diagnosis", *ACS Nano*, Vol. 15, No. 9, pp. 14207-14217, 2021.
[31] D. H. Kim, J. H. Cha, G. Shim, Y. H. Kim, J. S. Jang, H. Shin, J. Ahn, S. Y. Choi, and I. D. Kim, "Flash-thermochemical engineering of phase and surface activity on metal oxides", *Chem*, Vol. 8, No. 4, pp. 1014-1033, 2022.
[32] S. J. Joo, S. H. Park, C.vJ. Moon, and H. S. Kim, "A highly reliable copper nanowire/nanoparticle ink pattern with high conductivity on flexible substrate prepared via a flash light-sintering technique", *ACS Appl. Mater. Interfaces*, Vol. 7, No. 10, pp. 5674-5684, 2015.
[33] J. H. Cha, D. H. Kim, C. Park, S. J. Choi, J. S. Jang, S. Y. Yang, I. D. Kim, and S. Y. Choi, "Low-Thermal-Budget Doping of 2D Materials in Ambient Air Exemplified by Synthesis of Boron-Doped Reduced Graphene Oxide", *Adv. Sci.*, Vol. 7, No. 7, p. 1903318, 2020.